The Role of Unresolved PWNe to the Gamma-ray Diffuse Emission at GeV

Giulia Pagliaroli
Gran Sasso Science Institute, Italy

In collaboration with: V.Vecchiotti and F. L. Villante

Based on: https://doi.org/10.21203/rs.3.rs-539249/v1

OUTLINE

- Pulsar Wind Nebulae @ TeV
- The contribution of PWNe @ GeV
- The Fermi Unresolved PWNe
- Ring analysis of the diffuse gamma emission

PULSAR WIND NEBULAE @ TEV

The HGPS catalogue

of the HESS experiment is complete

for sources with $\Phi_i \geq 0.1\Phi_{CRAB}$

Abdalla et al, *A&A*, 612(2018)

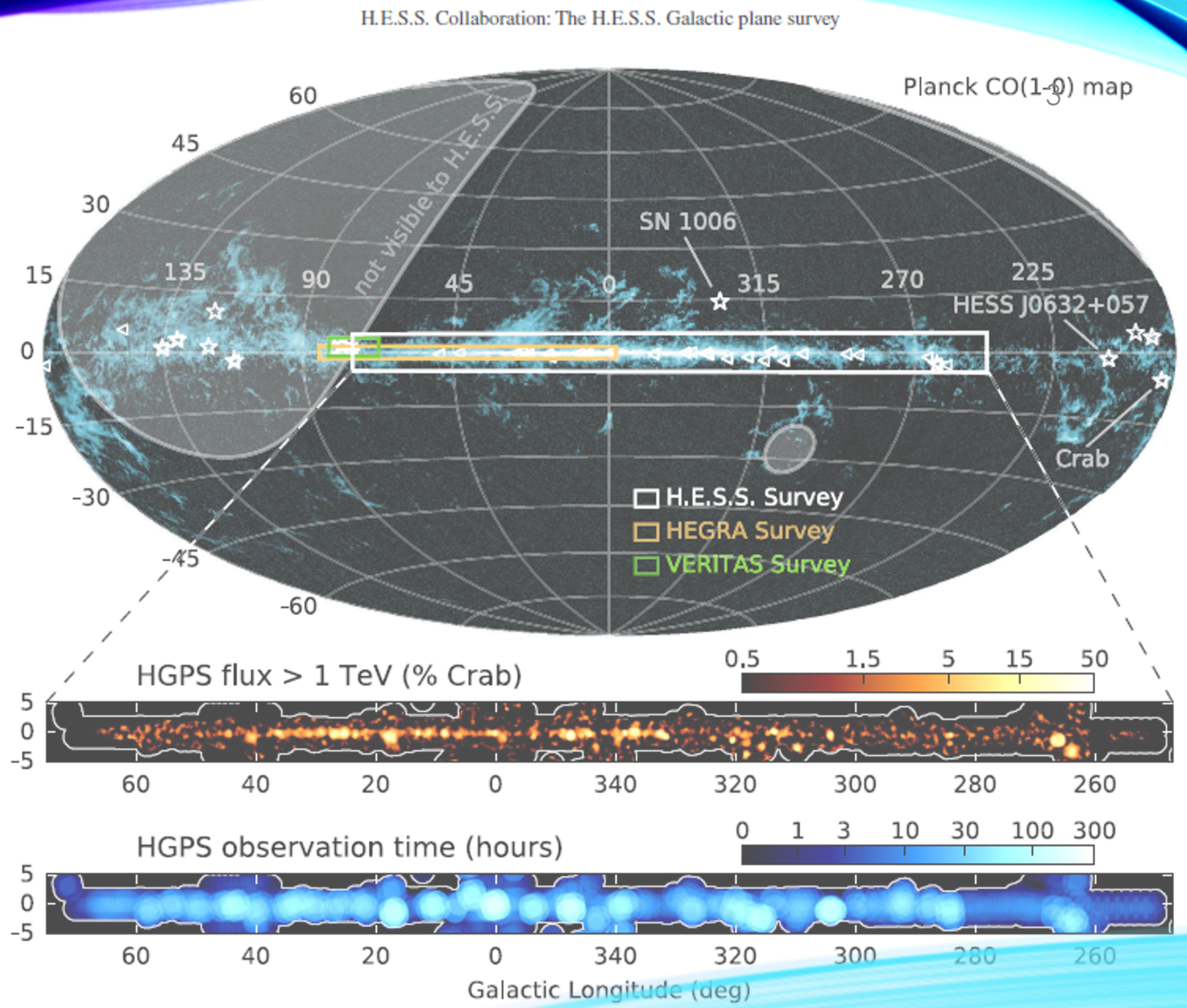

PWNe population study

Cataldo et al. *Astrophys.J.* 904 (2020)

See the ICRC talk of V. Vecchiotti

PULSARS POWERED

Pulsars Radial Distribution

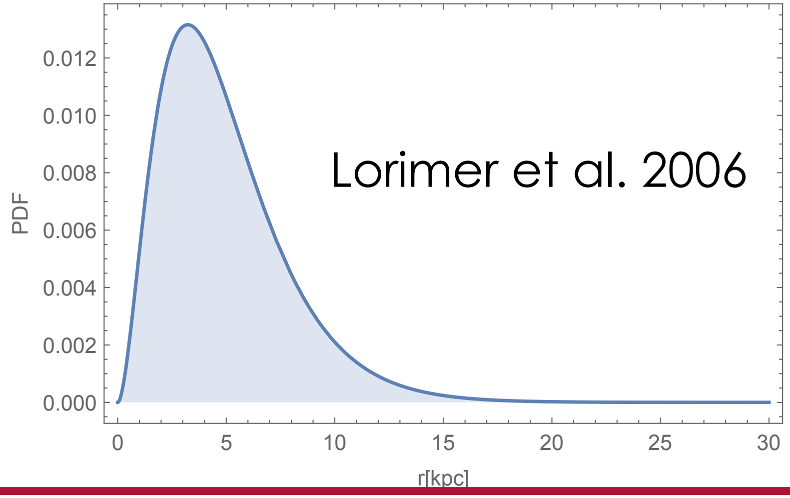

Cumulative distribution of PWNe

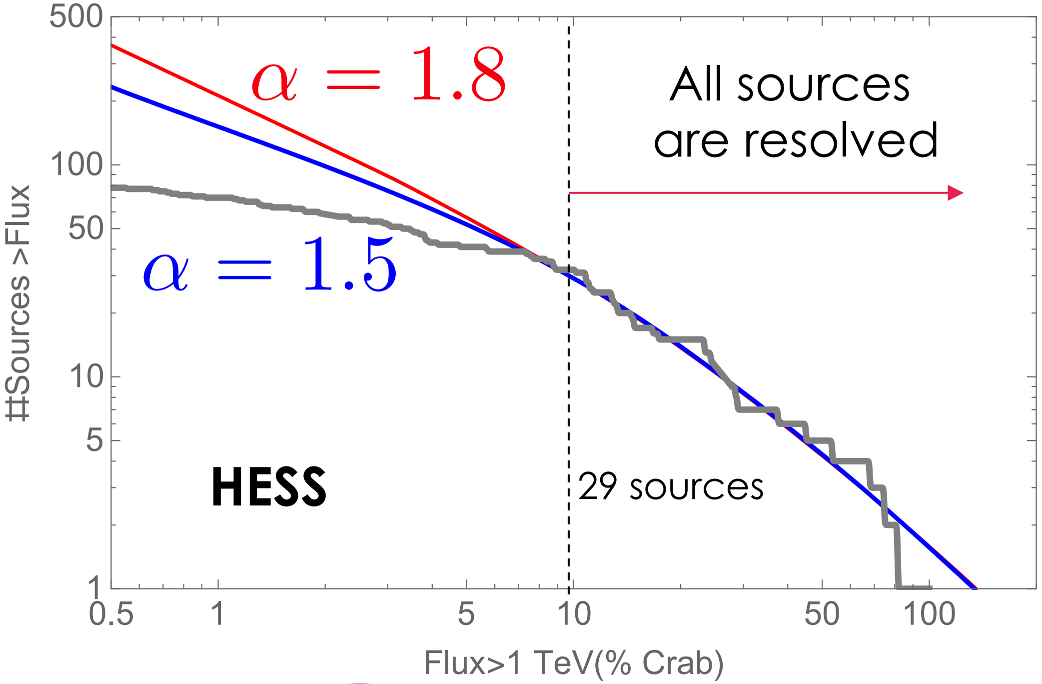

$$L(t) = L_{\max}\left(1 + \frac{t}{\tau}\right)^{-\gamma}$$

Luminosity Distribution

$$Y(L) = \frac{R\,\tau\,(\alpha - 1)}{L_{\max}}\left(\frac{L}{L_{\max}}\right)^{-\alpha}$$

$$\alpha = 1/\gamma + 1$$

$$R = 0.019\,\mathrm{yr}^{-1}$$

$$\frac{dN}{d^3r\,dL} = \rho(r)\,Y(L)$$

$$L_{\max}^{\mathrm{BF}},\ \tau^{\mathrm{BF}} \Rightarrow \Phi_{\mathrm{PWN}}$$

Total flux due to PWNe in the HESS energy range

$$\Phi_{\mathrm{TeV}} = \int_{1\mathrm{TeV}}^{100\mathrm{TeV}} dE\, \varphi_{PWN}(E)$$

$$\varphi_{\mathrm{PWN}}(E) \propto E^{-\beta_{\mathrm{TeV}}}$$

$$\beta_{\mathrm{TeV}} = 2.3$$

Average spectral index of HGPS

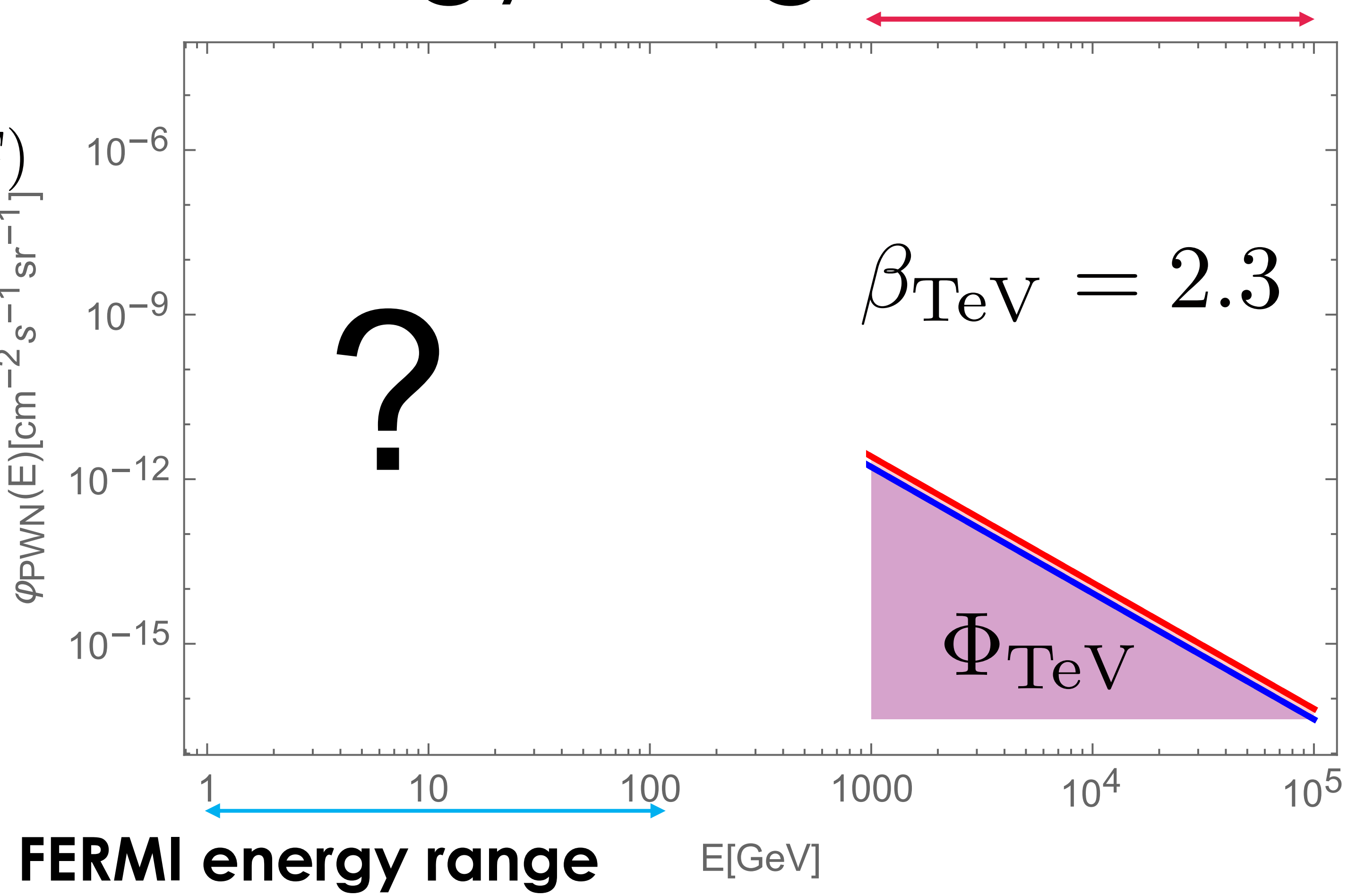

Total flux due to PWNe in the FERMI energy range

Total flux due to PWNe

Phenomenological prescription

$$\varphi_{\mathrm{PWN}} = \varphi_0 \begin{cases} \left(\frac{E}{E_b}\right)^{-\beta_{\mathrm{GeV}}} & E \leq E_b \\ \left(\frac{E}{E_b}\right)^{-\beta_{\mathrm{TeV}}} & E > E_b \end{cases}$$

$E_b = 300\mathrm{GeV}$

$\beta_{\mathrm{GeV}} < 2$

$$R_\Phi = \frac{\Phi_{\mathrm{GeV}}}{\Phi_{\mathrm{TeV}}}$$

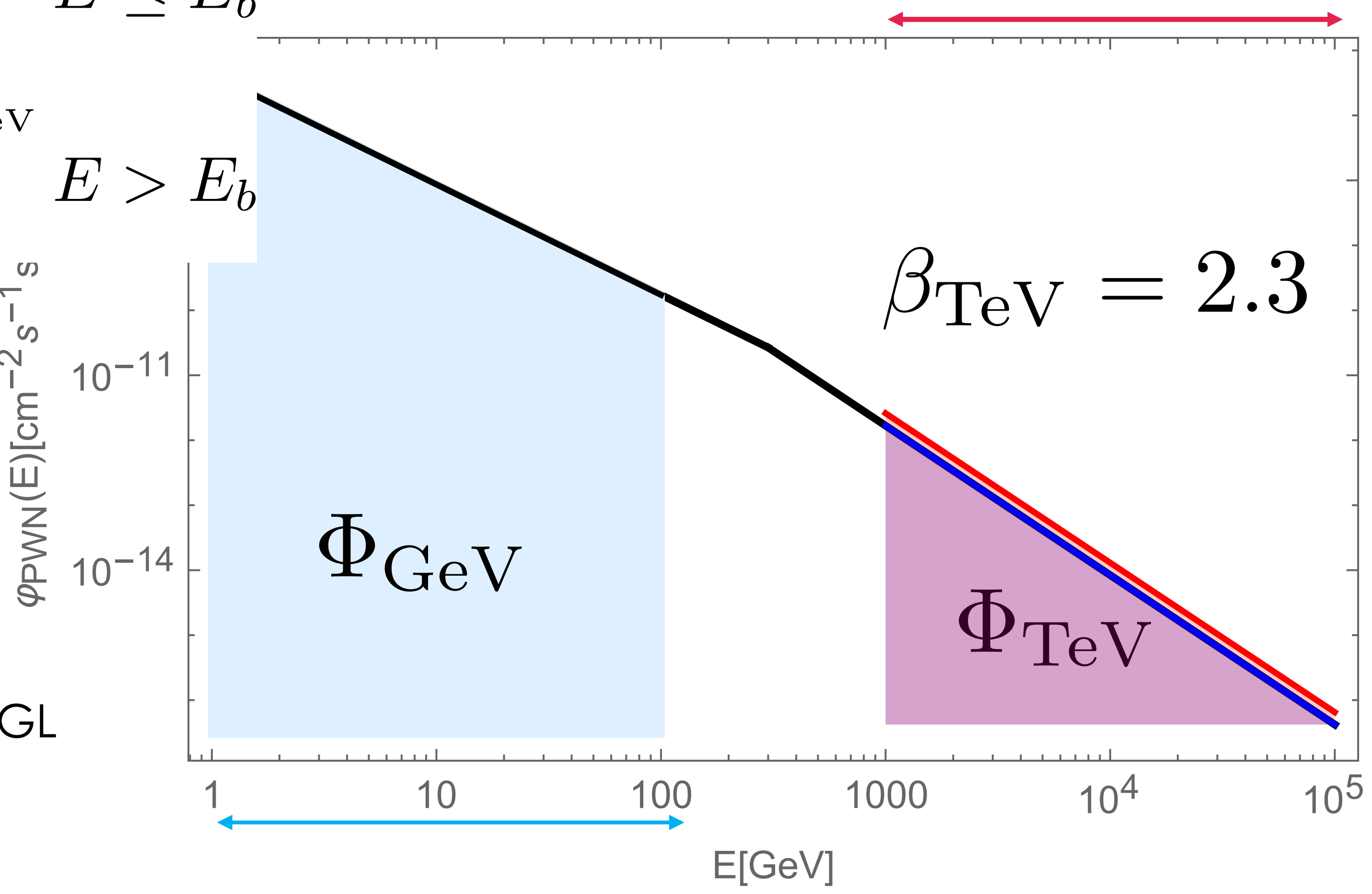

At least 3 arguments supporting it

- Consistency among HGPS and 3FGL
- Theoretical SED due to IC
- Observed PWNe flux ratios

Pulsar Wind Nebulae @ GeV energy

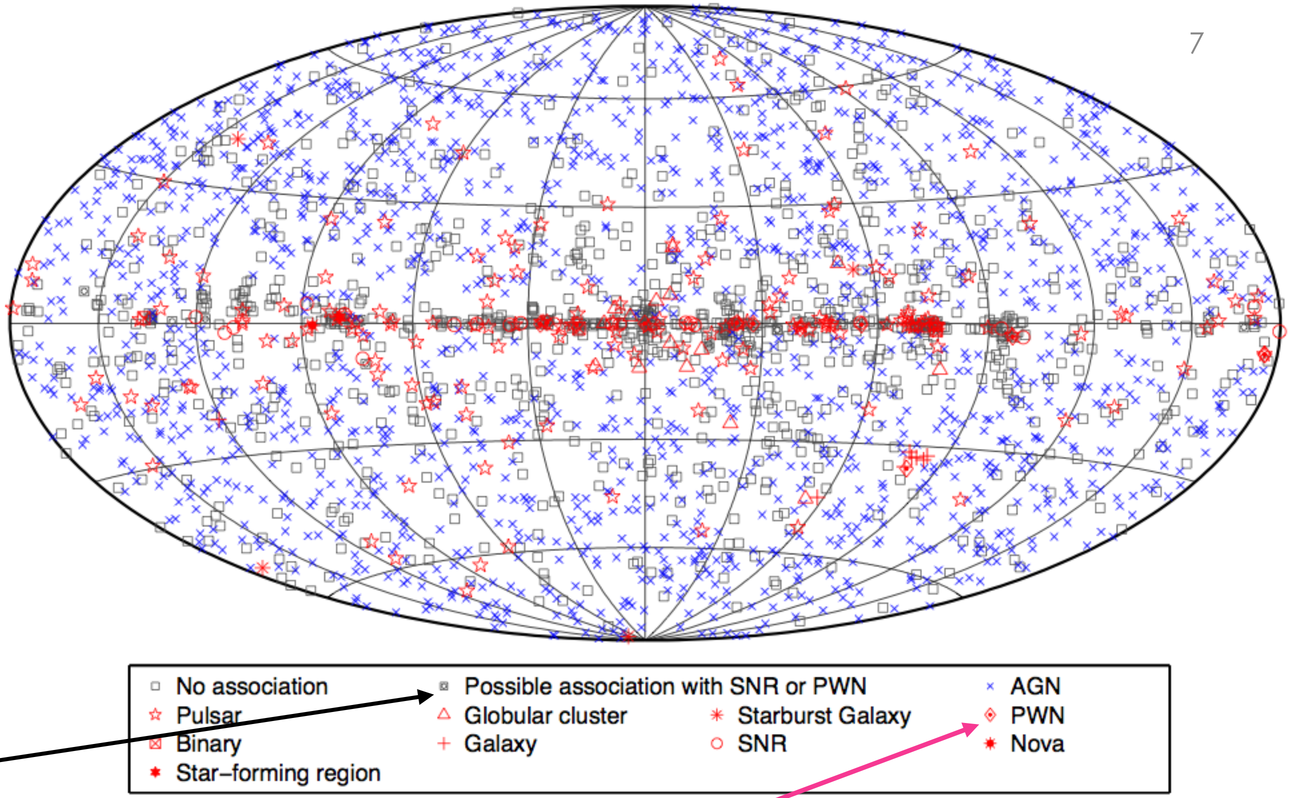

The 3FGL catalogue: 3033 sources

contains 45 spp (with possible association to PWNe) and 11 PWNe

Acero et.al. Astrophys.J.Suppl. 218 (2015)

Total Flux Due To PWNe In the FERMI Energy Range

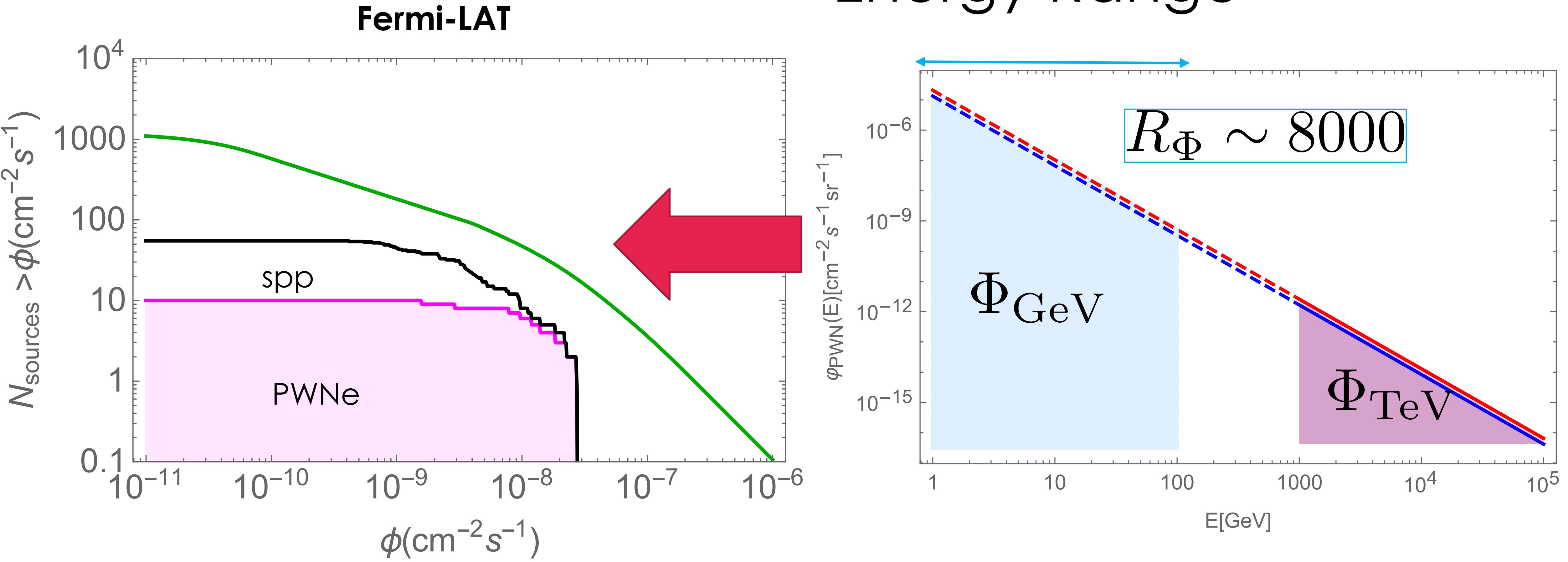

Expected cumulative distribution of Fermi-LAT PWNe under the assumption of spectral index $\beta_{GeV} = 2.3$

Total Flux Due To PWNe In the FERMI Energy Range

Ruled out by the non observation of very bright sources !

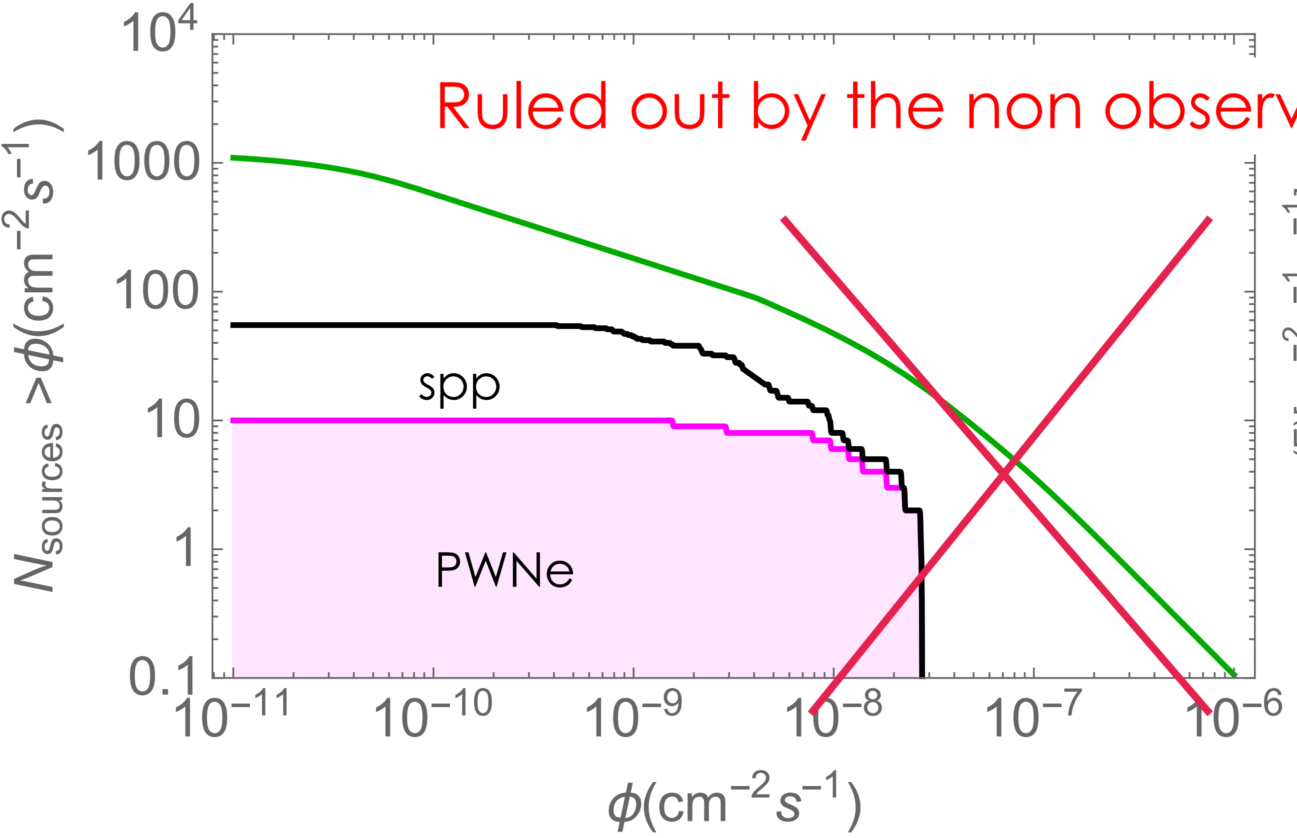

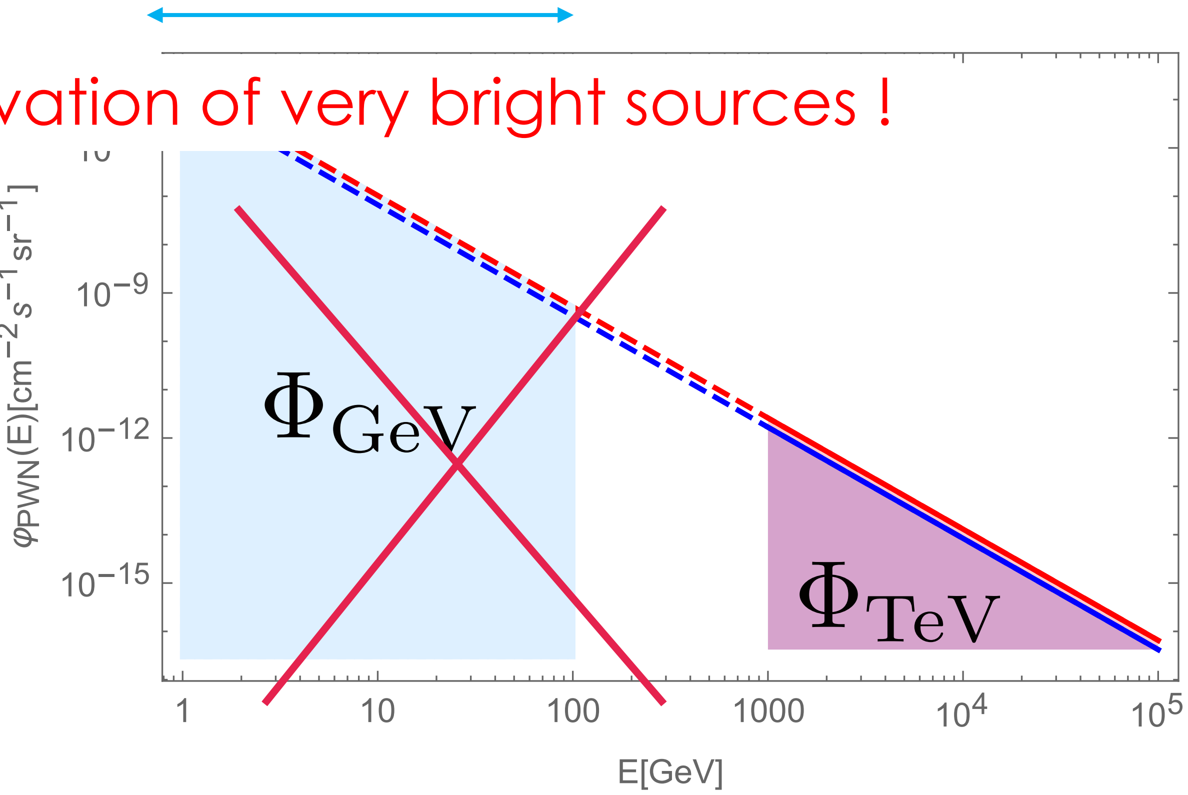

THEORETICAL EXPECTATIONS

Abdalla et.al.A&A612, A2(2018)

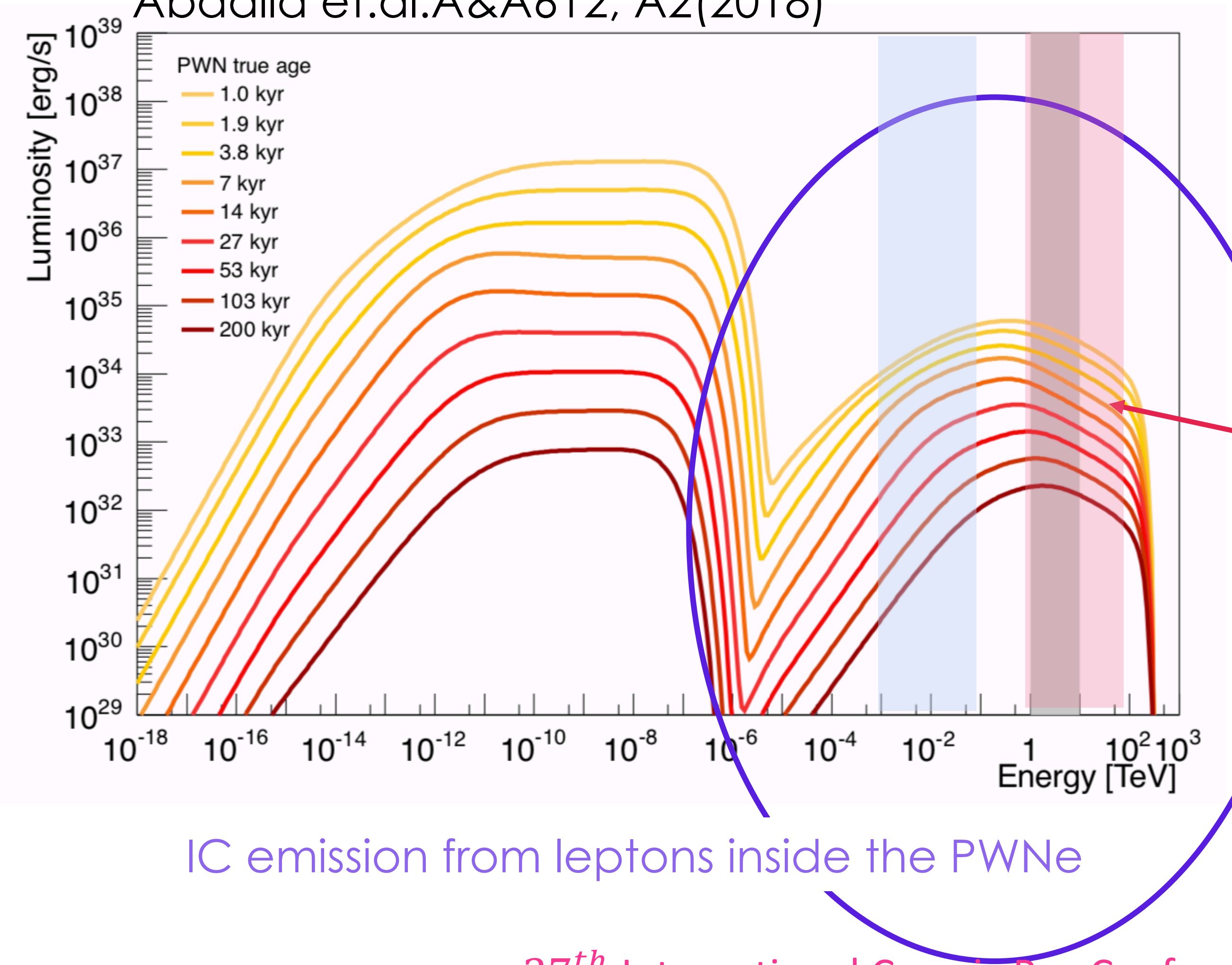

IC emission from leptons inside the PWNe

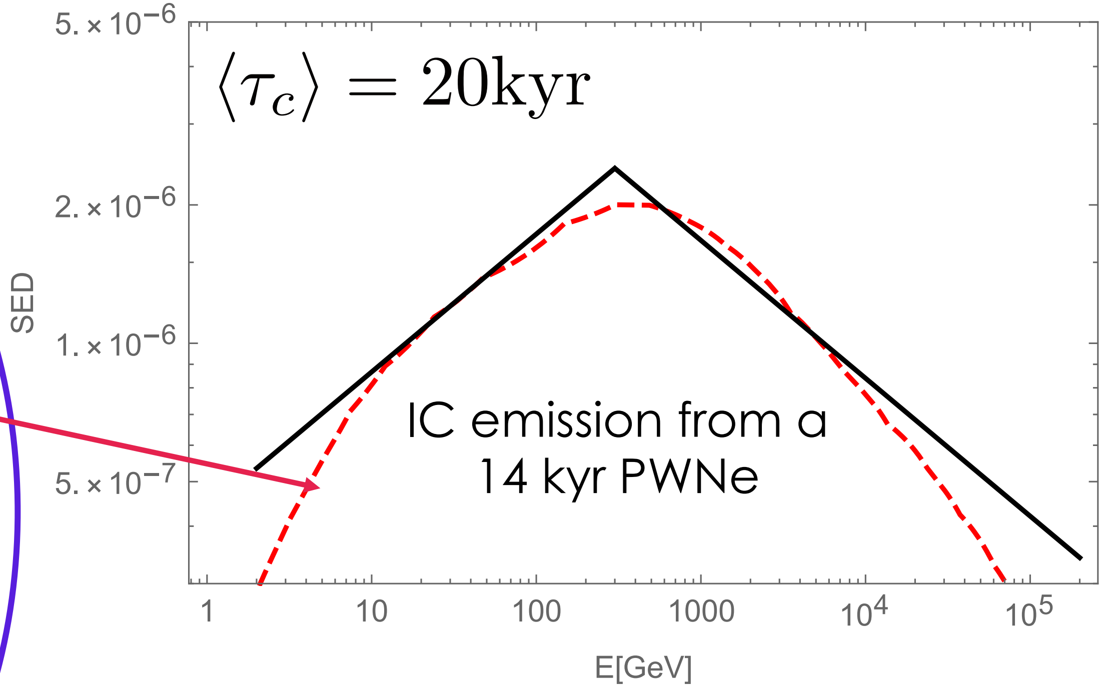

PWNe that are firmly identified both in the 3FGL and HGPS catalogues

- Only 6 objects:

HESS J1303-631, MSH 15-52, HESS J1616-508, HESS J1825-137, HESS J1837-069, HESS J1841-055

$$\langle R_\Phi \rangle \simeq 700$$

$$500 \leq R_\Phi \leq 1000$$

$$1.7 < \beta_{\mathrm{GeV}} < 1.9$$

Consistency among the HGPS and the 3FGL catalogues

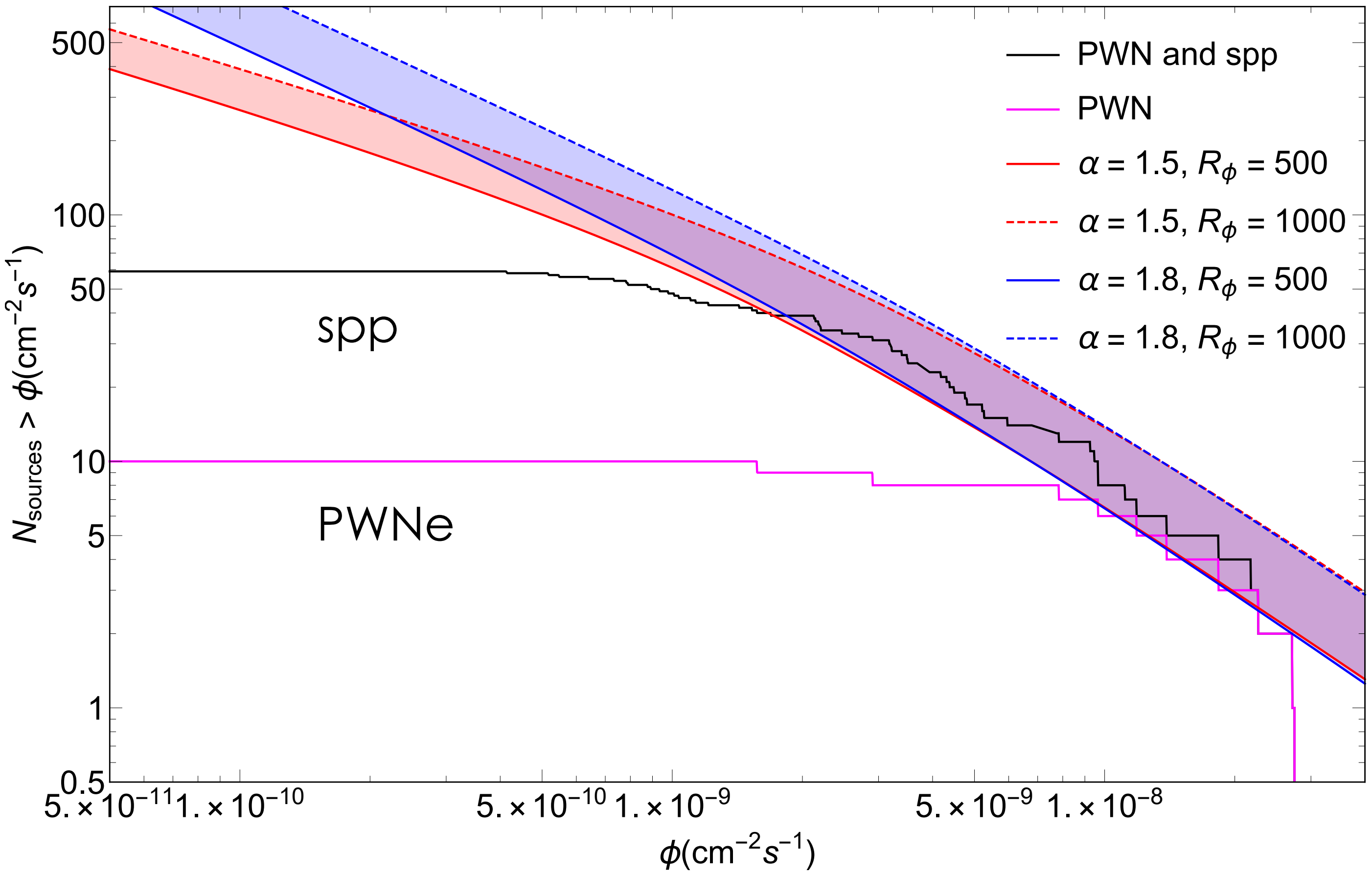

PWNe that are Unresolved by FERMI

$\alpha = 1.8 \quad R_\Phi = (500 - 1000)$

$$\frac{\Phi^{NR}}{\Phi_{PWN}} = (46\% - 40\%)$$

$\alpha = 1.5$

$$\frac{\Phi^{NR}}{\Phi_{PWN}} = (23\% - 17\%)$$

TAKE HOME MESSAGE #1

A relevant fraction of the TeV PWNe population cannot be resolved by Fermi-LAT

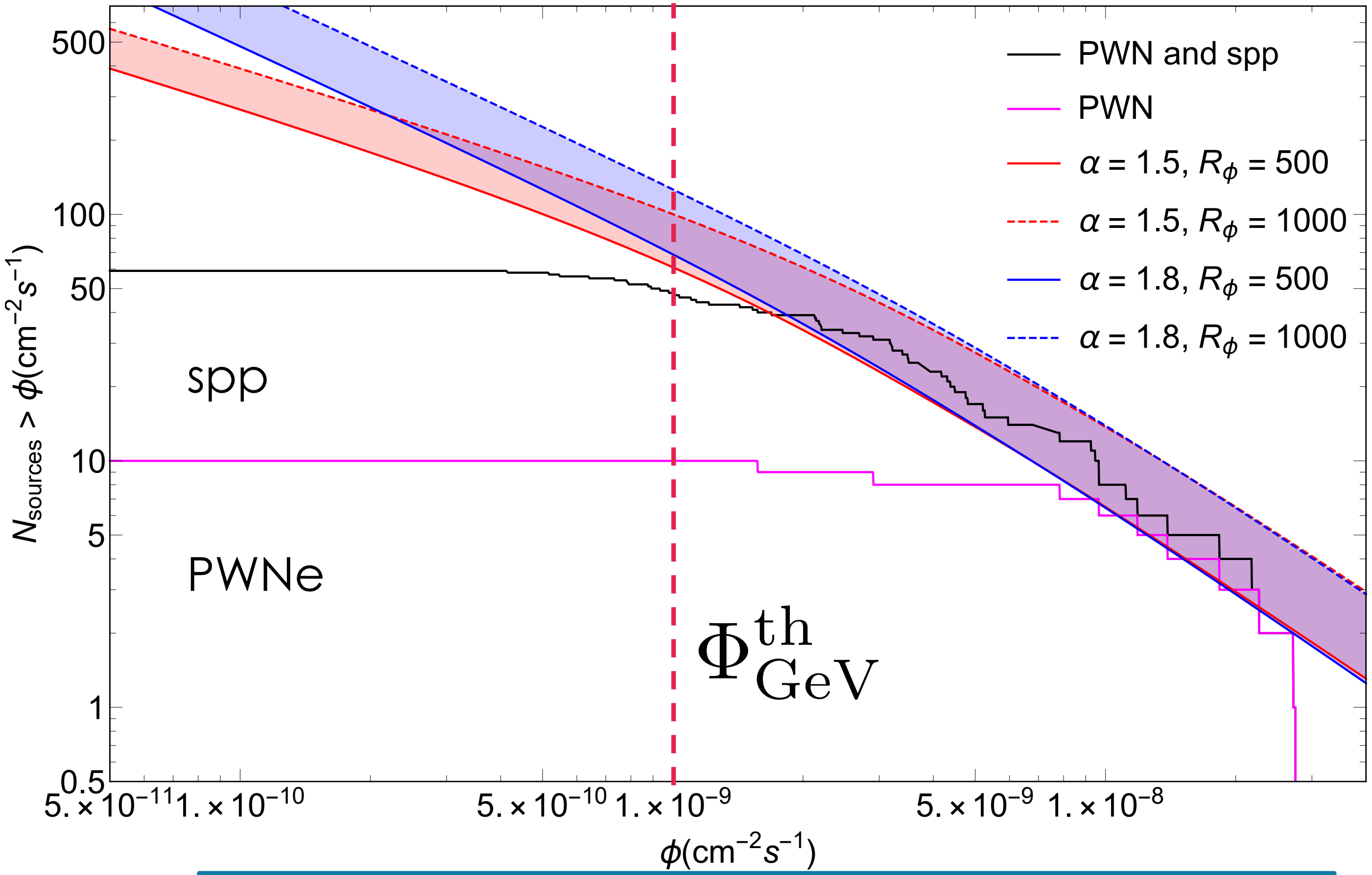

$$\Phi^{th}_{GeV} = 10^{-9}\,\mathrm{cm}^{-2}\,\mathrm{s}^{-1}$$ Acero et.al. 2015

IMPLICATIONS FOR THE FERMI DIFFUSE GAMMA-RAY EMISSION

Total diffuse emission=Truly diffuse emission due to CR interactions + cumulative flux due to Unresolved sources (**PWNe** +…)

TAKE HOME MESSAGE #2

Unresolved TeV PWNe and the truly diffuse emission, due to CRs interactions add up and shape the radial and spectral behaviours of the total diffuse γ-ray emission observed by Fermi-LAT

Ring analysis of FERMI diffuse emission

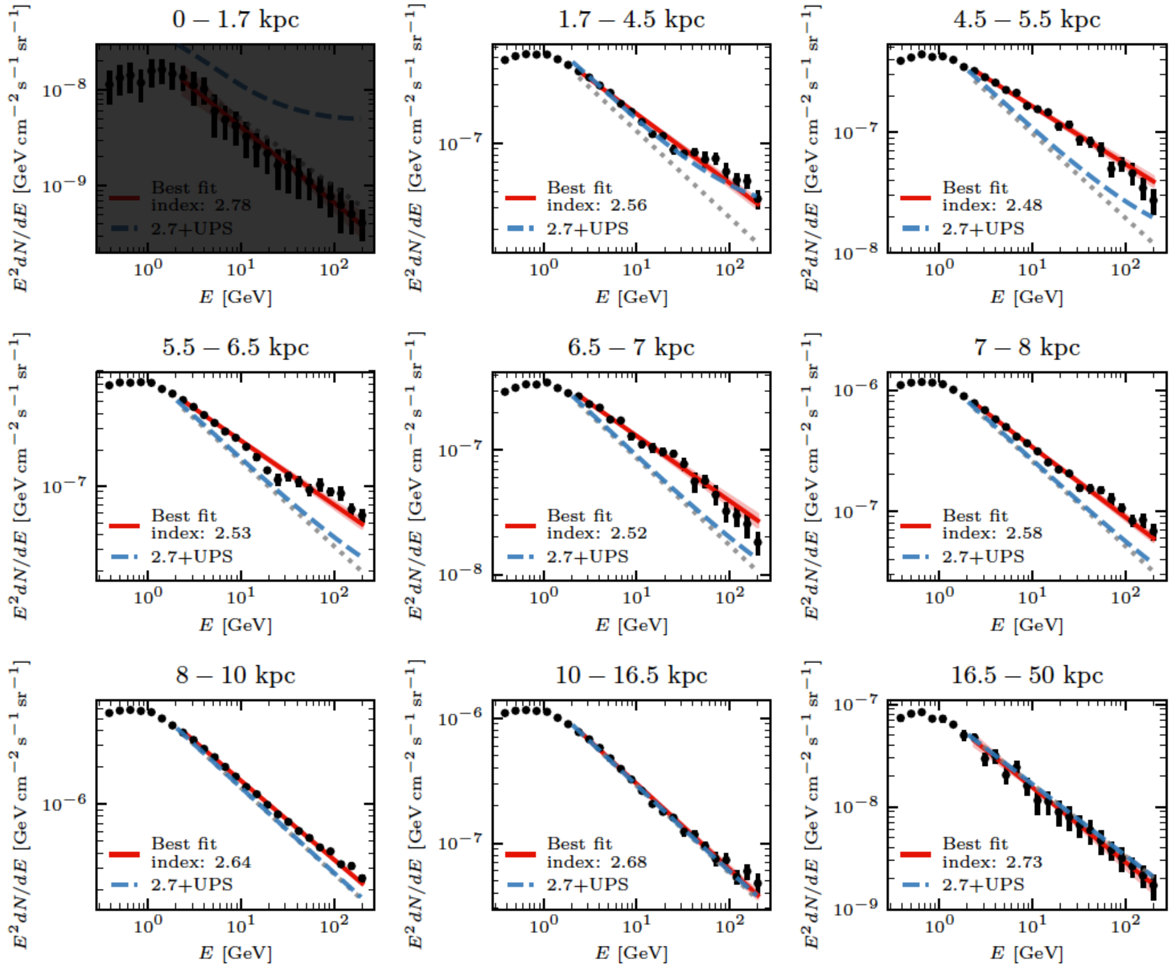

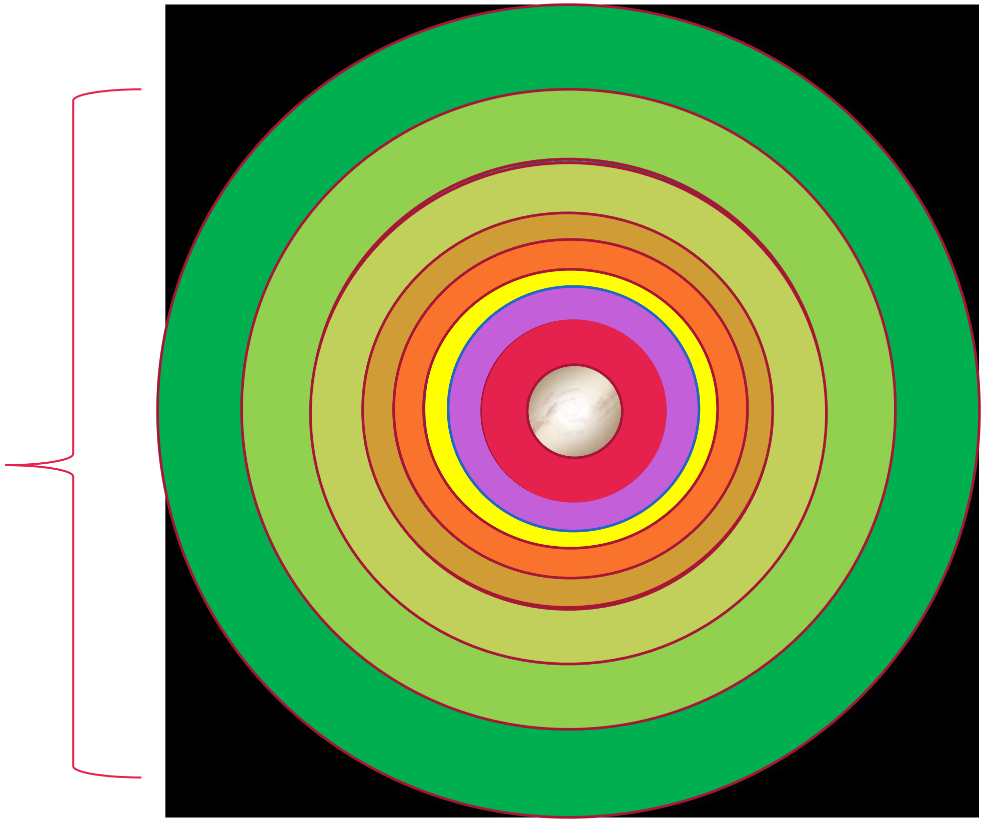

MILKY WAY

Total diffuse emission: 9.3 years of Fermi-LAT Pass 8 data (0.34−228.65) GeV and (|l|<180◦) and |b|<20.25◦

FERMI-LAT Data provided by Pothast et.al JCAP 2018

Total FERMI diffuse emission

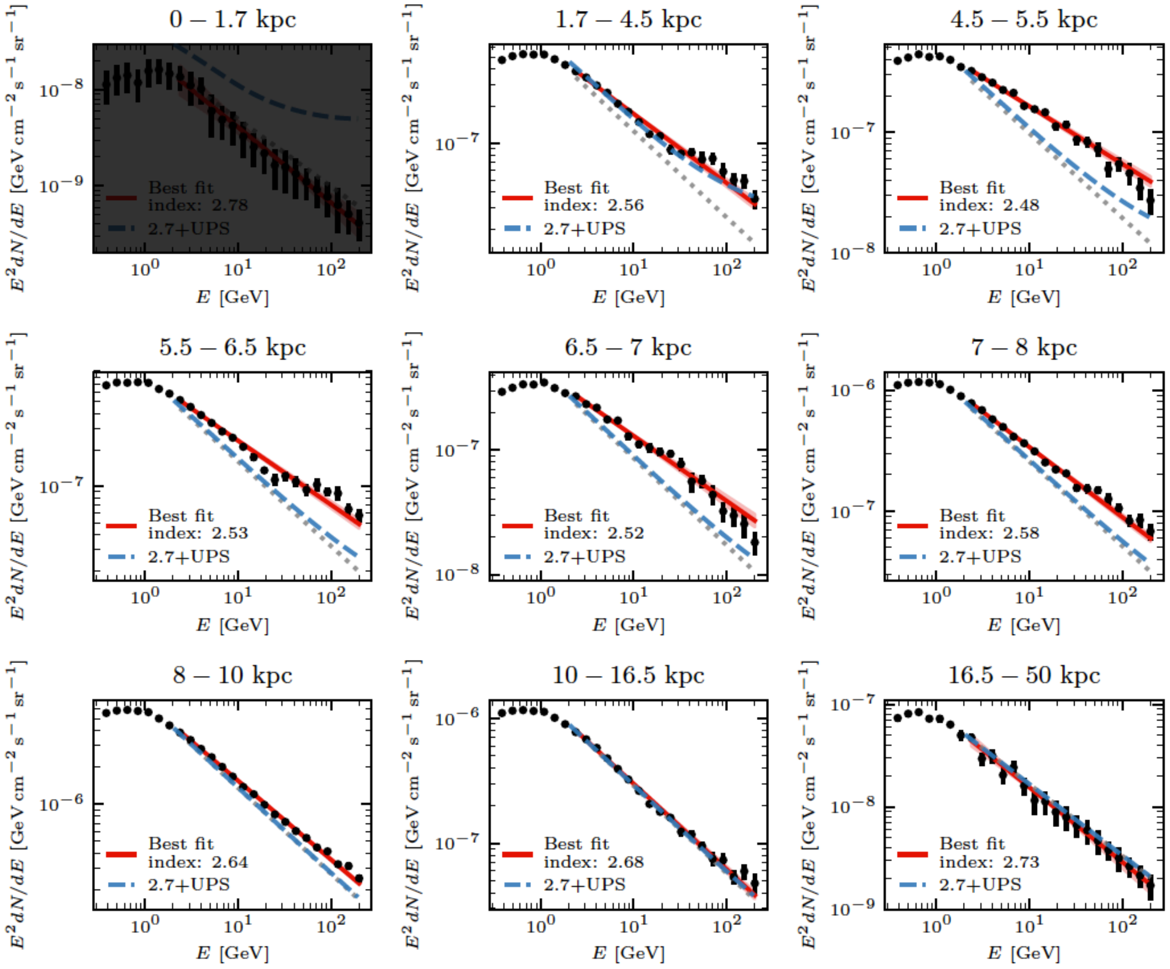

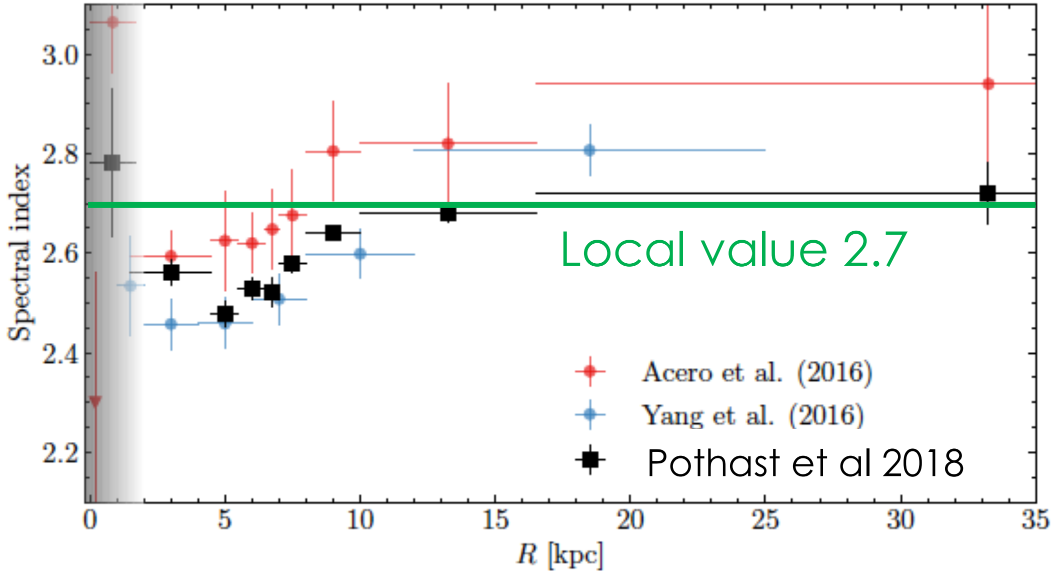

Indirect evidence of a progressive hardening of the CRs proton spectrum in the inner Galaxy

Total diffuse emission: 9.3 years of Fermi-LAT Pass 8 data (0.34−228.65) GeV and (|l|<180◦) and |b|<20.25◦

FERMI-LAT Data provided by Pothast et.al JCAP 2018

PWNe contribution in galactocentric rings

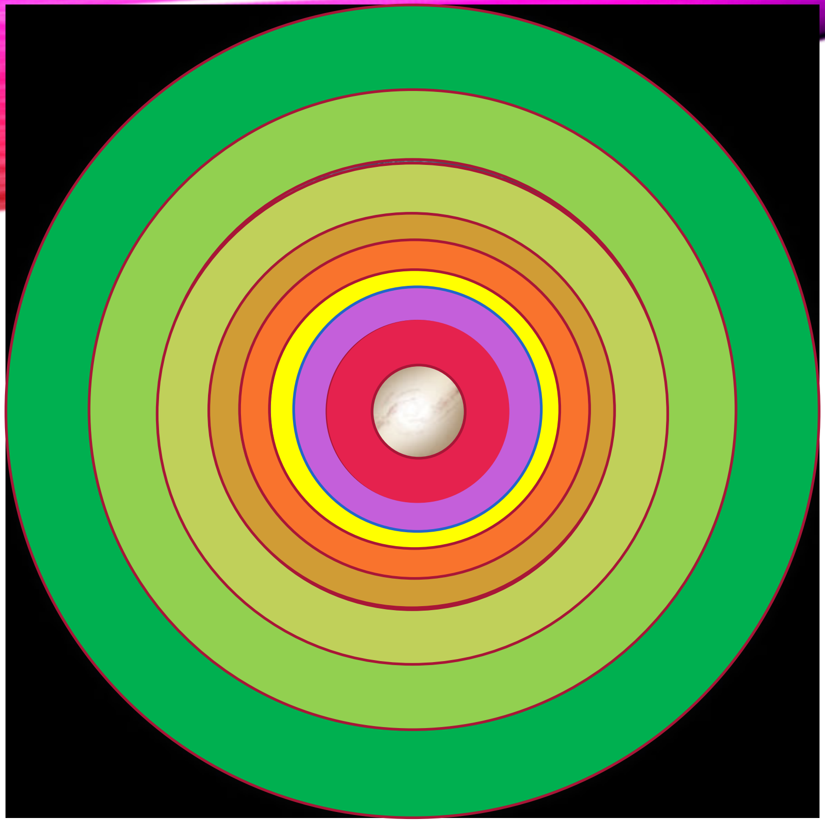

Table 1. *The cumulative flux of resolved (Φ^{R}_{GeV}) and unresolved (Φ^{NR}_{GeV}) TeV PWNe in the GeV domain for $\alpha = 1.8$ and for the two different values of R_Φ considered in our analysis. The Fermi-LAT diffuse emission Φ^{diff}_{GeV} is shown in the first column (Pothast et al. 2018). The numbers in brackets give the ratios $\Phi^{NR}_{GeV}/\Phi^{diff}_{GeV}$ in different galactocentric rings.*

	Φ^{diff}_{GeV} $(cm^{-2}\ s^{-1})$	Φ^{NR}_{GeV} $(cm^{-2}\ s^{-1})$		Φ^{R}_{GeV} $(cm^{-2}\ s^{-1})$	
		$R_\Phi = 500$	$R_\Phi = 1000$	$R_\Phi = 500$	$R_\Phi = 1000$
1.7 – 4.5 kpc	3.86×10^{-7}	6.63×10^{-8} (17%)	1.15×10^{-7} (29.9%)	2.78×10^{-8}	7.29×10^{-8}
4.5 – 5.5 kpc	3.11×10^{-7}	3.8×10^{-8} (12.2%)	6.62×10^{-8} (21.2%)	2.1×10^{-8}	5.2×10^{-8}
5.5 – 6.5 kpc	5.09×10^{-7}	4.24×10^{-8} (8.3%)	7.37×10^{-8} (14.4%)	3.0×10^{-8}	7.14×10^{-8}
6.5 – 7.0 kpc	2.57×10^{-7}	2.28×10^{-8} (8.8%)	3.96×10^{-8} (15.3%)	2.08×10^{-8}	4.77×10^{-8}
7.0 – 8.0 kpc	7.7×10^{-7}	5.29×10^{-8} (6.8%)	9.21×10^{-8} (11.9%)	7.03×10^{-8}	1.54×10^{-7}
8.0 – 10.0 kpc	3.84×10^{-6}	9.69×10^{-8} (2.5%)	1.68×10^{-7} (4.3%)	2.24×10^{-7}	4.74×10^{-7}
10.0 – 16.5 kpc	7.68×10^{-7}	3.0×10^{-8} (3.9%)	5.24×10^{-8} (6.8%)	1.9×10^{-8}	4.56×10^{-8}
16.5 – 50.0 kpc	4.44×10^{-8}	7.73×10^{-10} (1.7%)	1.38×10^{-9} (3.1%)	9.23×10^{-11}	3.44×10^{-10}
0.0 – 50.0 kpc	6.89×10^{-6}	3.55×10^{-7}(5.1%)	6.18×10^{-7} (8.9%)	4.15×10^{-7}	9.23×10^{-7}

9 Galactocentric rings

Total diffuse emission: 9.3 years of Fermi-LAT Pass 8 data (0.34−228.65) GeV and (|l|<180◦) and |b|<20.25◦

Diffuse emission due to unresolved PWNe @(1-100) GeV

Resolved flux due to PWNe

REINTERPRETING THE DIFFUSE EMISSION OBSERVED BY FERMI

Table 1. *The cumulative flux of resolved (Φ^{R}_{GeV}) and unresolved (Φ^{NR}_{GeV}) TeV PWNe in the GeV domain for $\alpha = 1.8$ and for the two different values of R_{Φ} considered in our analysis. The Fermi-LAT diffuse emission Φ^{diff}_{GeV} is shown in the first column (Pothast et al. 2018). The numbers in brackets give the ratios $\Phi^{NR}_{GeV}/\Phi^{diff}_{GeV}$ in different galactocentric rings.*

	Φ^{diff}_{GeV} $(cm^{-2}\ s^{-1})$	Φ^{NR}_{GeV} $(cm^{-2}\ s^{-1})$		Φ^{R}_{GeV} $(cm^{-2}\ s^{-1})$	
		$R_{\Phi} = 500$	$R_{\Phi} = 1000$	$R_{\Phi} = 500$	$R_{\Phi} = 1000$
1.7 – 4.5 kpc	3.86×10^{-7}	6.63×10^{-8} (17%)	1.15×10^{-7} (29.9%)	2.78×10^{-8}	7.29×10^{-8}
4.5 – 5.5 kpc	3.11×10^{-7}	3.8×10^{-8} (12.2%)	6.62×10^{-8} (21.2%)	2.1×10^{-8}	5.2×10^{-8}
5.5 – 6.5 kpc	5.09×10^{-7}	4.24×10^{-8} (8.3%)	7.37×10^{-8} (14.4%)	3.0×10^{-8}	7.14×10^{-8}
6.5 – 7.0 kpc	2.57×10^{-7}	2.28×10^{-8} (8.8%)	3.96×10^{-8} (15.3%)	2.08×10^{-8}	4.77×10^{-8}
7.0 – 8.0 kpc	7.7×10^{-7}	5.29×10^{-8} (6.8%)	9.21×10^{-8} (11.9%)	7.03×10^{-8}	1.54×10^{-7}
8.0 – 10.0 kpc	3.84×10^{-6}	9.69×10^{-8} (2.5%)	1.68×10^{-7} (4.3%)	2.24×10^{-7}	4.74×10^{-7}
10.0 – 16.5 kpc	7.68×10^{-7}	3.0×10^{-8} (3.9%)	5.24×10^{-8} (6.8%)	1.9×10^{-8}	4.56×10^{-8}
16.5 – 50.0 kpc	4.44×10^{-8}	7.73×10^{-10} (1.7%)	1.38×10^{-9} (3.1%)	9.23×10^{-11}	3.44×10^{-10}
0.0 – 50.0 kpc	6.89×10^{-6}	3.55×10^{-7}(5.1%)	6.18×10^{-7} (8.9%)	4.15×10^{-7}	9.23×10^{-7}

REINTERPRETING THE DIFFUSE EMISSION OBSERVED BY FERMI

Dashed-green line: best-fit power-law of FERMI data without the PWNe contribution

$$\Gamma_1 = 2.56$$

Thick green line: best-fit power-law of the truly diffuse emission due to CRs

$$\Gamma_{BF} = 2.72$$

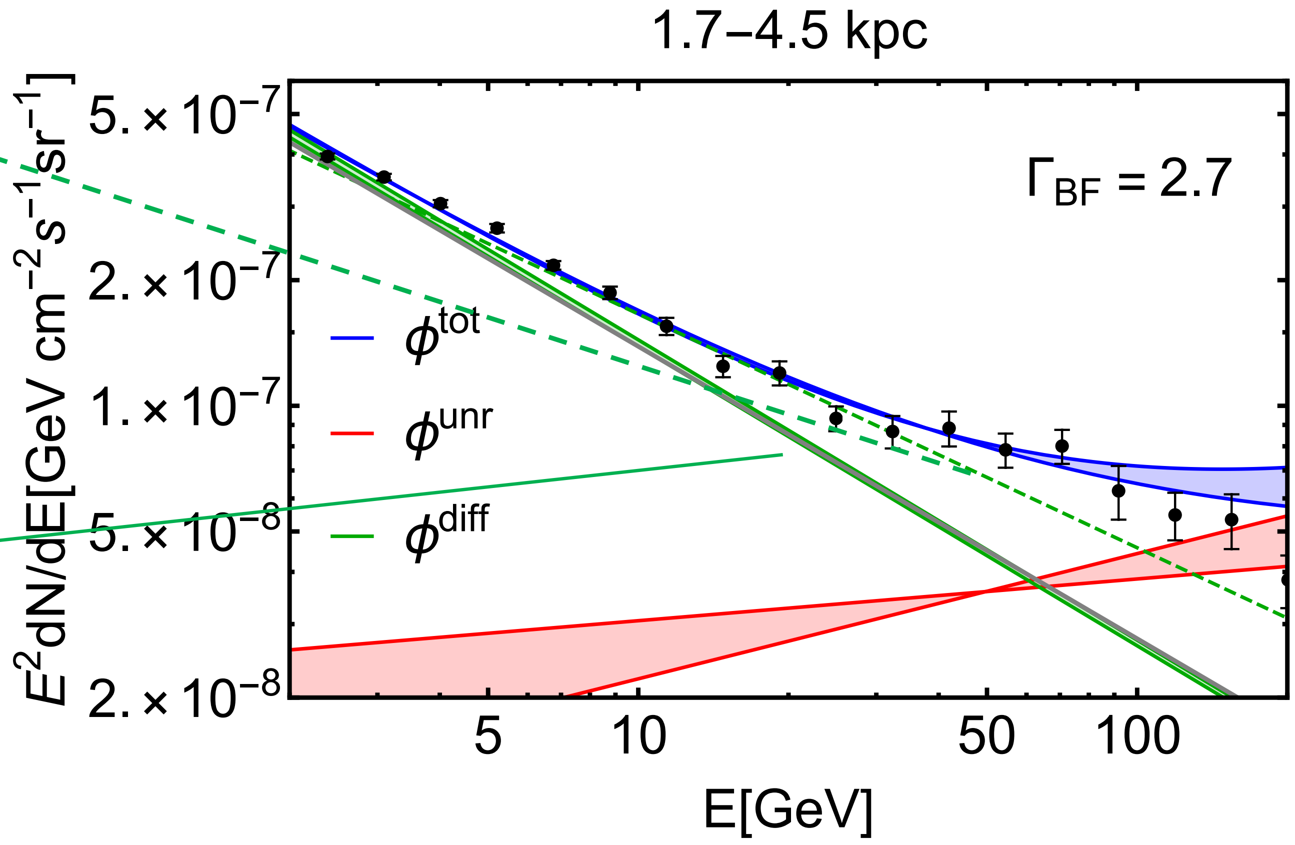

Spectral index of the truly diffuse emission due to CRs

Table 2. *Spectral indexes of the CR diffuse emission obtained by fitting the Fermi-LAT data with (Γ_{BF}) and without (Γ_1) TeV PWNe unresolved contribution. The indexes Γ_1 coincide with those obtained by Pothast et al. (2018).*

Ring	Γ_1	Γ_{BF} $R_\Phi = 500$	$\alpha = 1.8$ $R_\Phi = 1000$
$1.7 - 4.5$ kpc	2.56 ± 0.02	2.72 ± 0.01	2.72 ± 0.01
$4.5 - 5.5$ kpc	2.48 ± 0.02	2.57 ± 0.01	2.56 ± 0.01
$5.5 - 6.5$ kpc	2.54 ± 0.04	2.63 ± 0.01	2.63 ± 0.01
$6.5 - 7$ kpc	2.54 ± 0.01	2.62 ± 0.01	2.61 ± 0.02
$7 - 8$ kpc	2.57 ± 0.01	2.625 ± 0.008	2.623 ± 0.008
$8 - 10$ kpc	2.642 ± 0.003	2.663 ± 0.003	2.662 ± 0.004
$10 - 16.5$ kpc	2.696 ± 0.008	2.743 ± 0.008	2.740 ± 0.009
$16.5 - 50$ kpc	2.72 ± 0.03	2.77 ± 0.04	2.76 ± 0.03

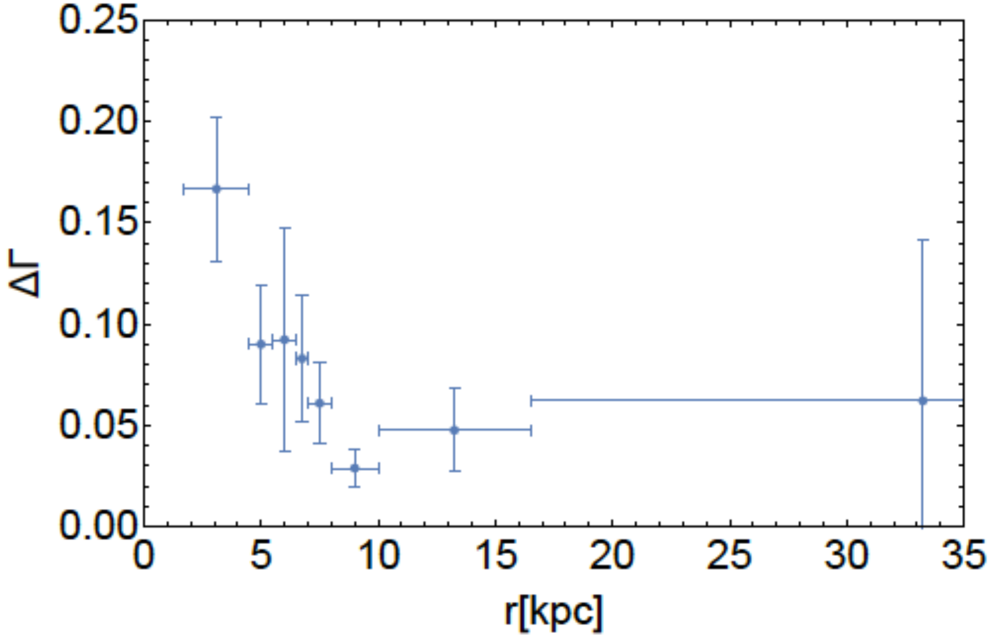

Figure 2. *The difference $\Delta\Gamma$ between the spectral index of the truly diffuse emission obtained in different Galactocentric rings by fitting the Fermi-LAT data with/without the contribution of unresolved PWNe.*

TAKE HOME MESSAGE #3

PWNe contribution accounts for a large part of the spectral index variation observed by Fermi-LAT, weakening the evidence of CR spectral hardening in the inner Galaxy

SUMMARY

1. A relevant fraction of the TeV PWNe population cannot be resolved by Fermi-LAT
2. The γ-ray flux due to unresolved TeV PWNe and the truly diffuse emission, due to CRs interactions with the interstellar gas, add up contributing to shape the radial and spectral behaviour of the total diffuse γ-ray emission observed by Fermi-LAT
3. This additional component naturally accounts for a large part of the spectral index variation observed by Fermi-LAT, weakening the evidence of CR spectral hardening in the inner Galaxy

Based on: https://doi.org/10.21203/rs.3.rs-539249/v1

Gray line: speculative diffuse component with spectral index fixed to 2.7 normalized in order to interpolate the data at 1 GeV

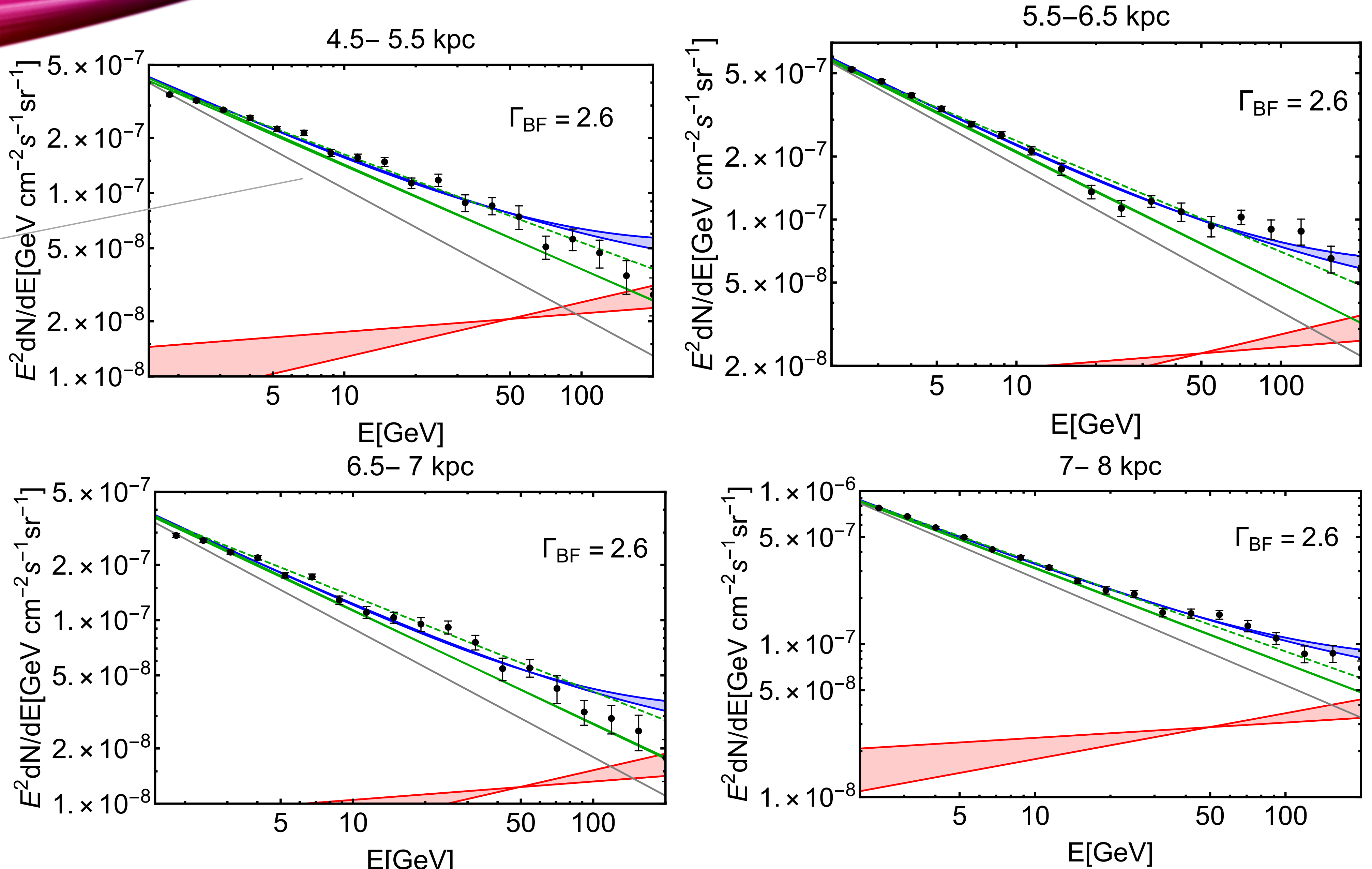

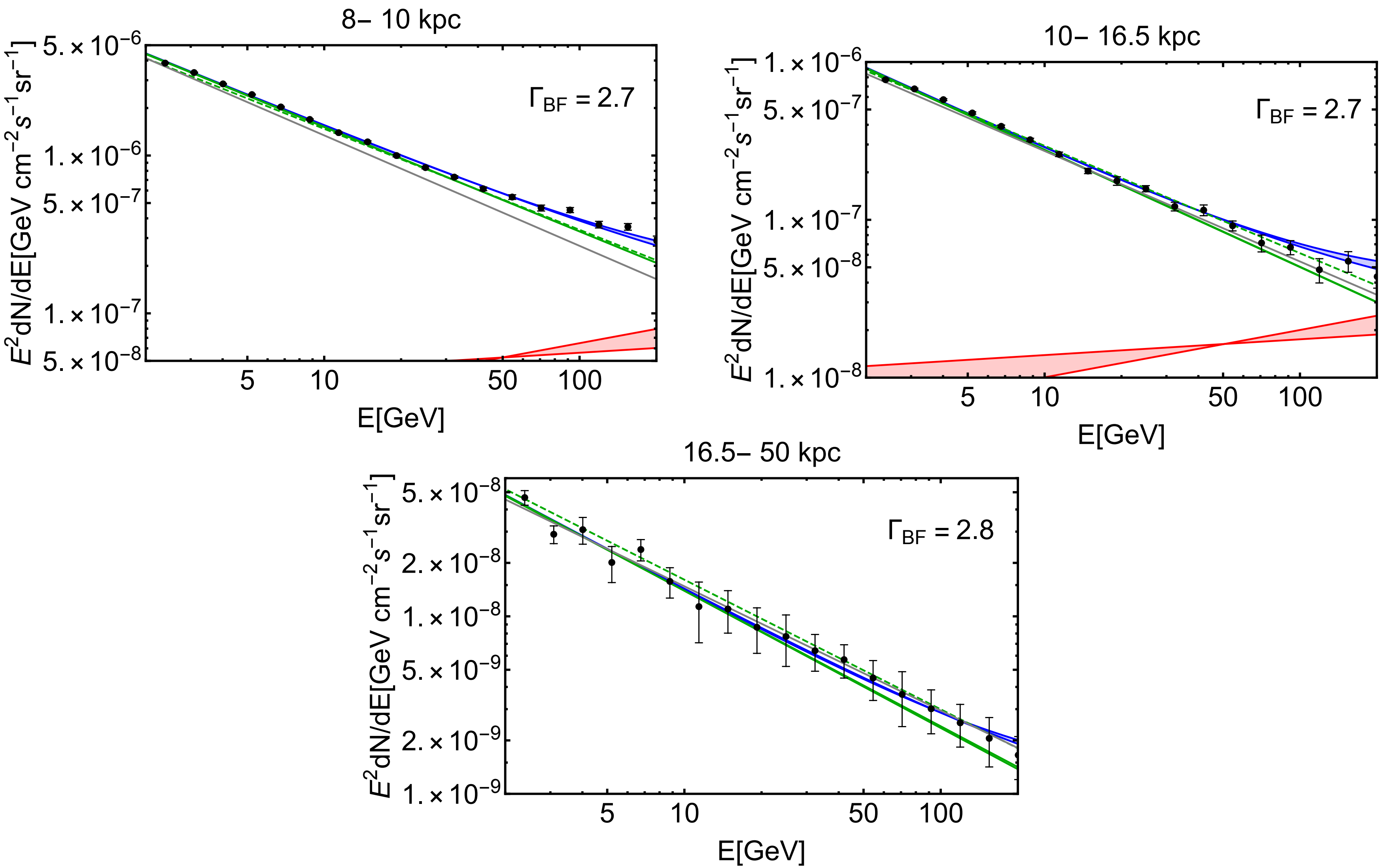

8– 10 kpc
Γ_BF = 2.7
E²dN/dE[GeV cm⁻²s⁻¹sr⁻¹]
5.×10⁻⁶
1.×10⁻⁶
5.×10⁻⁷
1.×10⁻⁷
5.×10⁻⁸
5
10
50
100
E[GeV]
10– 16.5 kpc
Γ_BF = 2.7
E²dN/dE[GeV cm⁻²s⁻¹sr⁻¹]
1.×10⁻⁶
5.×10⁻⁷
1.×10⁻⁷
5.×10⁻⁸
1.×10⁻⁸
5
10
50
100
E[GeV]
16.5– 50 kpc
Γ_BF = 2.8
E²dN/dE[GeV cm⁻²s⁻¹sr⁻¹]
5.×10⁻⁸
2.×10⁻⁸
1.×10⁻⁸
5.×10⁻⁹
2.×10⁻⁹
1.×10⁻⁹
5
10
50
100
E[GeV]

Model:

The power-law for the luminosity distribution can be automatically obtained assuming a fading source population (like PWNe, TeV Halos) create at a constant rate $\bar{r}$.

The spin-down power is described by: $\dot{E}(t) = \dot{E}_0 \left(1 + \frac{t}{\tau}\right)^{-2}$

Considering that a fraction $\boldsymbol{\lambda(t)}$ of the spin-down power is converted into gamma-rays then the intrinsic luminosity decreases according to:

$$L(t) = \lambda(t)\dot{E}(t) = \lambda\dot{E}_0 \left(1 + \frac{t}{\tau}\right)^{-\gamma} \text{ where } \gamma = 2(\delta + 1);$$

$\boldsymbol{L_{max}}$

$$\lambda(t) = \lambda \left(\frac{\dot{E}(t)}{\dot{E}_0}\right)^{\delta}$$

Abdalla et al, *A&A*, 612, A2 (2018)

Then:

$$Y(L) = \frac{\bar{r}\,\tau\,(\alpha - 1)}{L_{\max}} \left(\frac{L}{L_{\max}}\right)^{-\alpha}$$

Where $\bar{r} = 0.019\ yr^{-1}$ is the SN's rate and $\alpha = \left(\frac{1}{\gamma} + 1\right)$ therefore for $\gamma = 2$ we have $\alpha = 1.5$.

And instead of the parameter $\mathcal{N}$ we have the spin-down timescale of the Pulsar τ.

PWNe that are Unresolved by FERMI

Upper limit by Fermi for the total unresolved component:3%

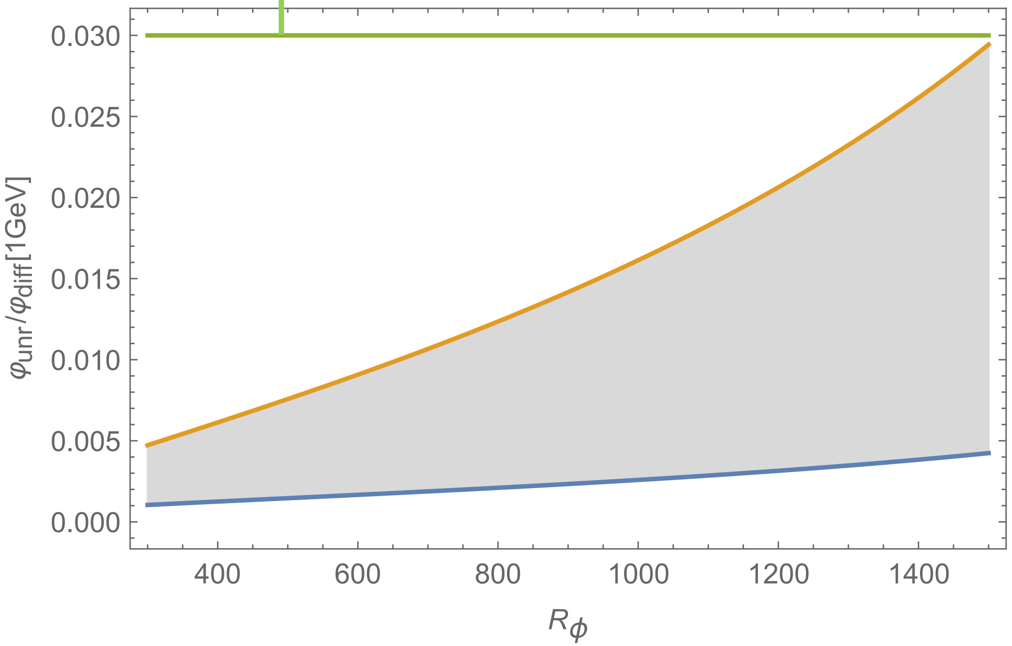

Negligible at 1 GeV increases with energy and could be as large as the 30% of the total γ-ray diffuse emission at 100 GeV

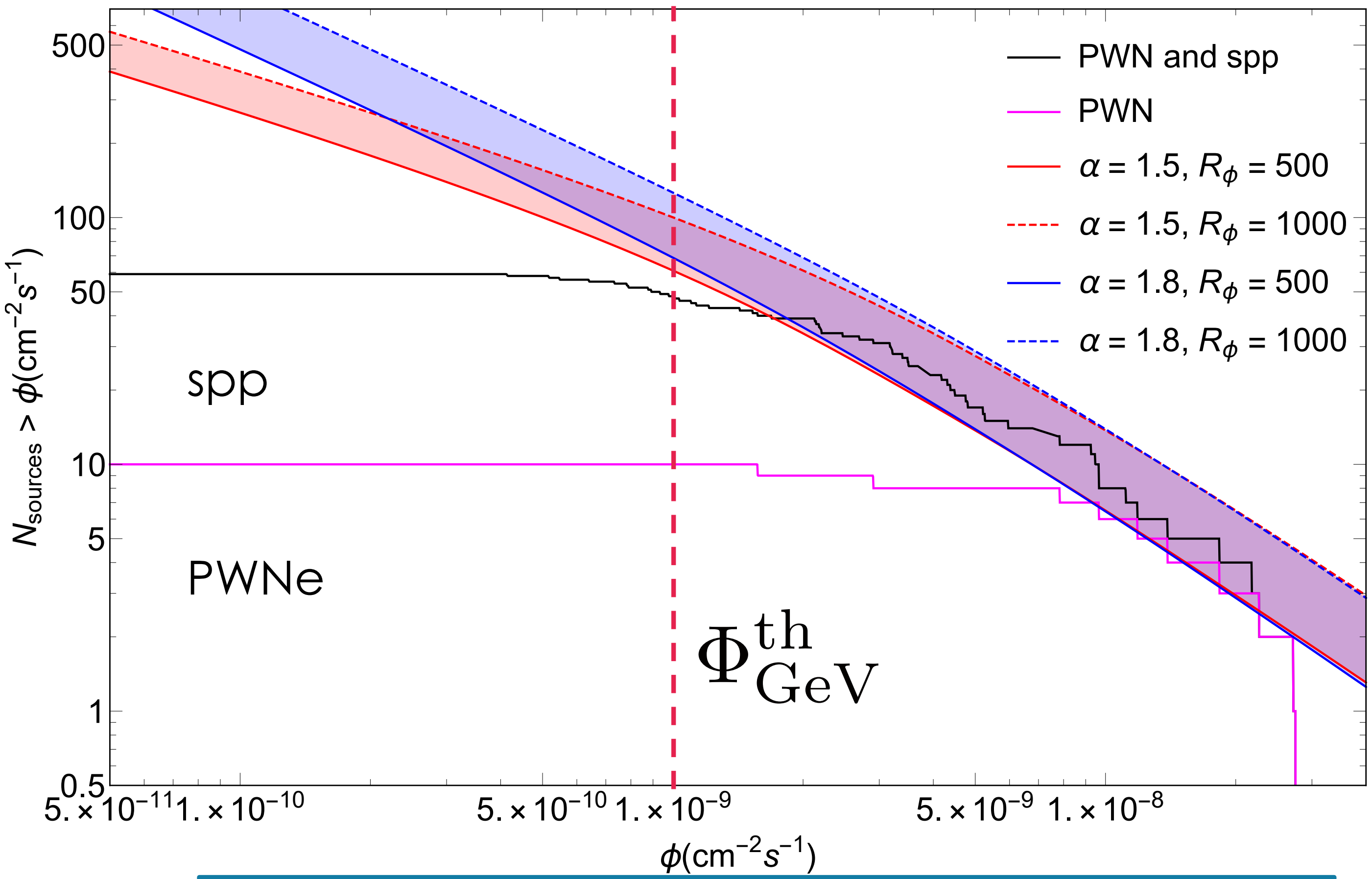

$$\Phi^{th}_{GeV} = 10^{-9}\,\mathrm{cm}^{-2}\,\mathrm{s}^{-1}$$ Acero et.al. 2015

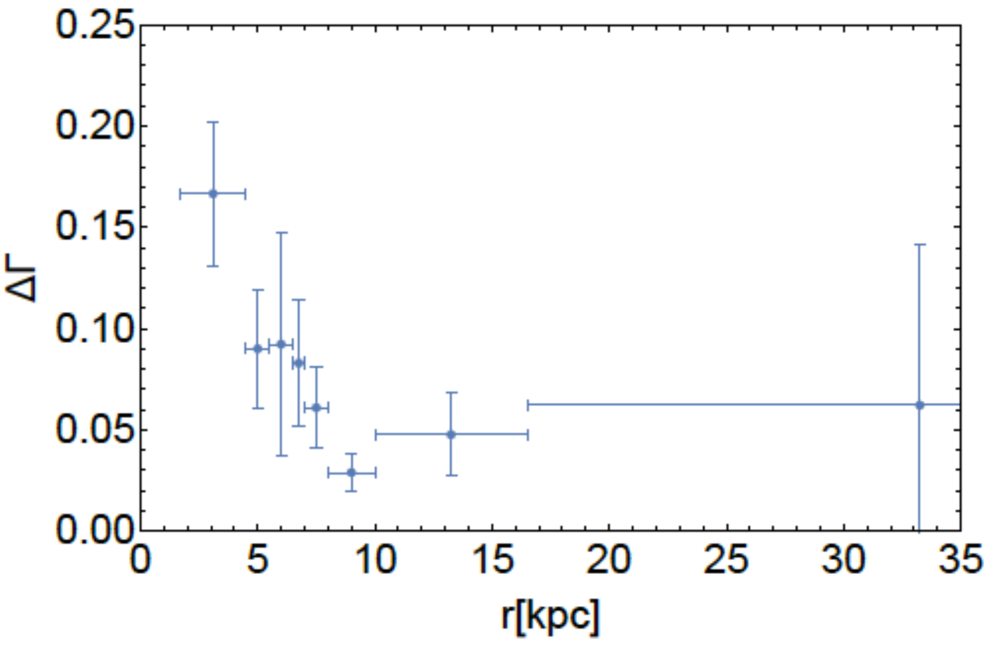

Figure 2. *The difference ΔΓ between the spectral index of the truly diffuse emission obtained in different Galactocentric rings by fitting the Fermi-LAT data with/without the contribution of unresolved PWNe.*

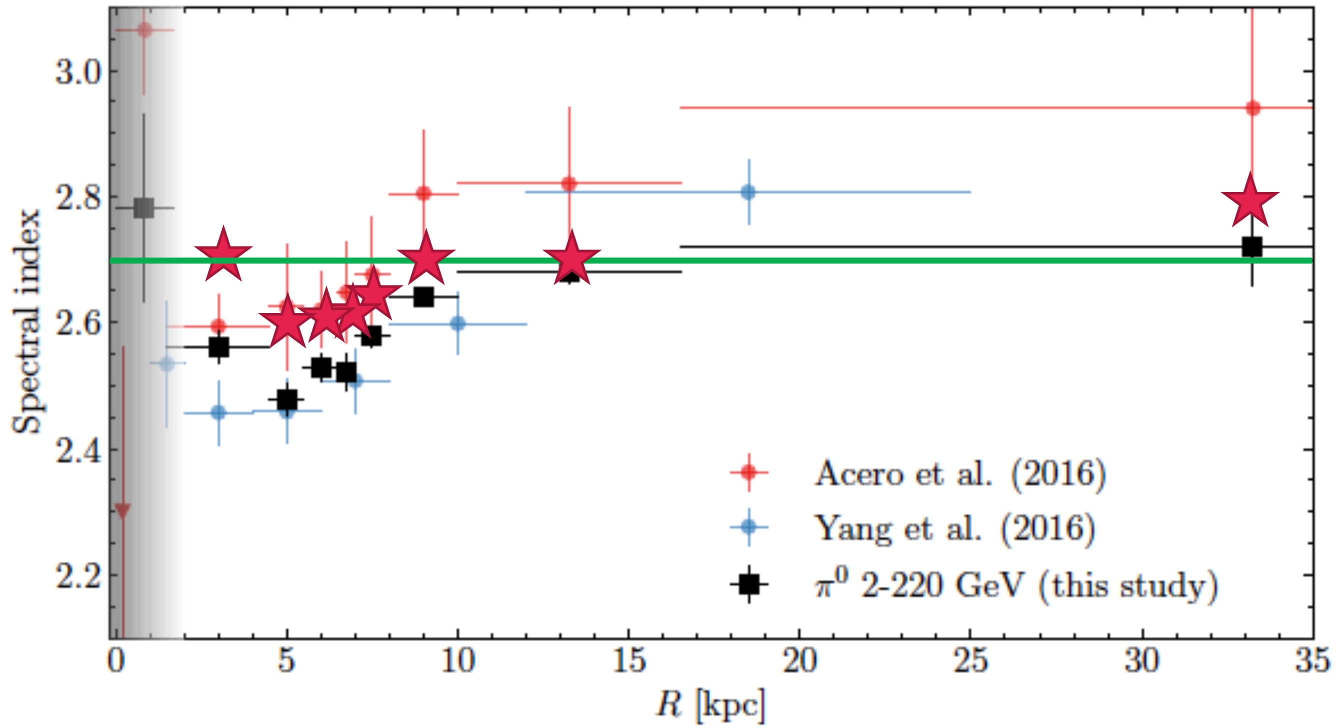

RING RESULTS FOR ALPHA=1.5

Table 2. *We provide the cumulative flux of resolved (Φ^{R}_{GeV}) and unresolved (Φ^{NR}_{GeV}) TeV PWNe in the GeV domain for $\alpha = 1.5$ and for two different values of R_{Φ} taken into account in our analysis. It is shown in bracket the percentage of unresolved sources with respect to the total diffuse γ-ray emission measured by Fermi-LAT in each galactocentric ring.*

	Φ^{NR}_{GeV} $(cm^{-2}\ s^{-1})$		Φ^{R}_{GeV} $(cm^{-2}\ s^{-1})$	
	$R_{\Phi} = 500$	$R_{\Phi} = 1000$	$R_{\Phi} = 500$	$R_{\Phi} = 1000$
1.7 – 4.5 kpc	3.37×10^{-8} (8.7%)	4.76×10^{8} (12.3%)	3.41×10^{-8}	8.8×10^{-8}
4.5 – 5.5 kpc	1.75×10^{-8} (5.6%)	2.47×10^{-8} (7.9%)	2.50×10^{-8}	6.04×10^{-8}
5.5 – 6.5 kpc	1.76×10^{-8} (3.4%)	2.48×10^{-8} (4.9%)	3.47×10^{-8}	7.97×10^{-8}
6.5 – 7.0 kpc	8.31×10^{-9} (3.2%)	1.17×10^{-8} (4.5%)	2.31×10^{-8}	5.12×10^{-8}
7.0 – 8.0 kpc	1.58×10^{-8} (2.0%)	2.24×10^{-8} (2.9%)	7.29×10^{-8}	1.55×10^{-7}
8.0 – 10.0 kpc	2.27×10^{-8} (0.6%)	3.25×10^{-8} (0.8%)	2.08×10^{-7}	4.3×10^{-7}
10.0 – 16.5 kpc	1.35×10^{-8} (1.8%)	2.00×10^{-8} (2.6%)	2.18×10^{-8}	5.06×10^{-8}
16.5 – 50.0 kpc	5.23×10^{-10} (2.1%)	8.37×10^{-10} (1.9%)	1.00×10^{-10}	4.1×10^{-10}
0.0 – 50.0 kpc	1.32×10^{-7}(1.9%)	1.88×10^{-7} (2.7%)	4.22×10^{-7}	9.22×10^{-7}

RESULTS FOR ALPHA=1.5

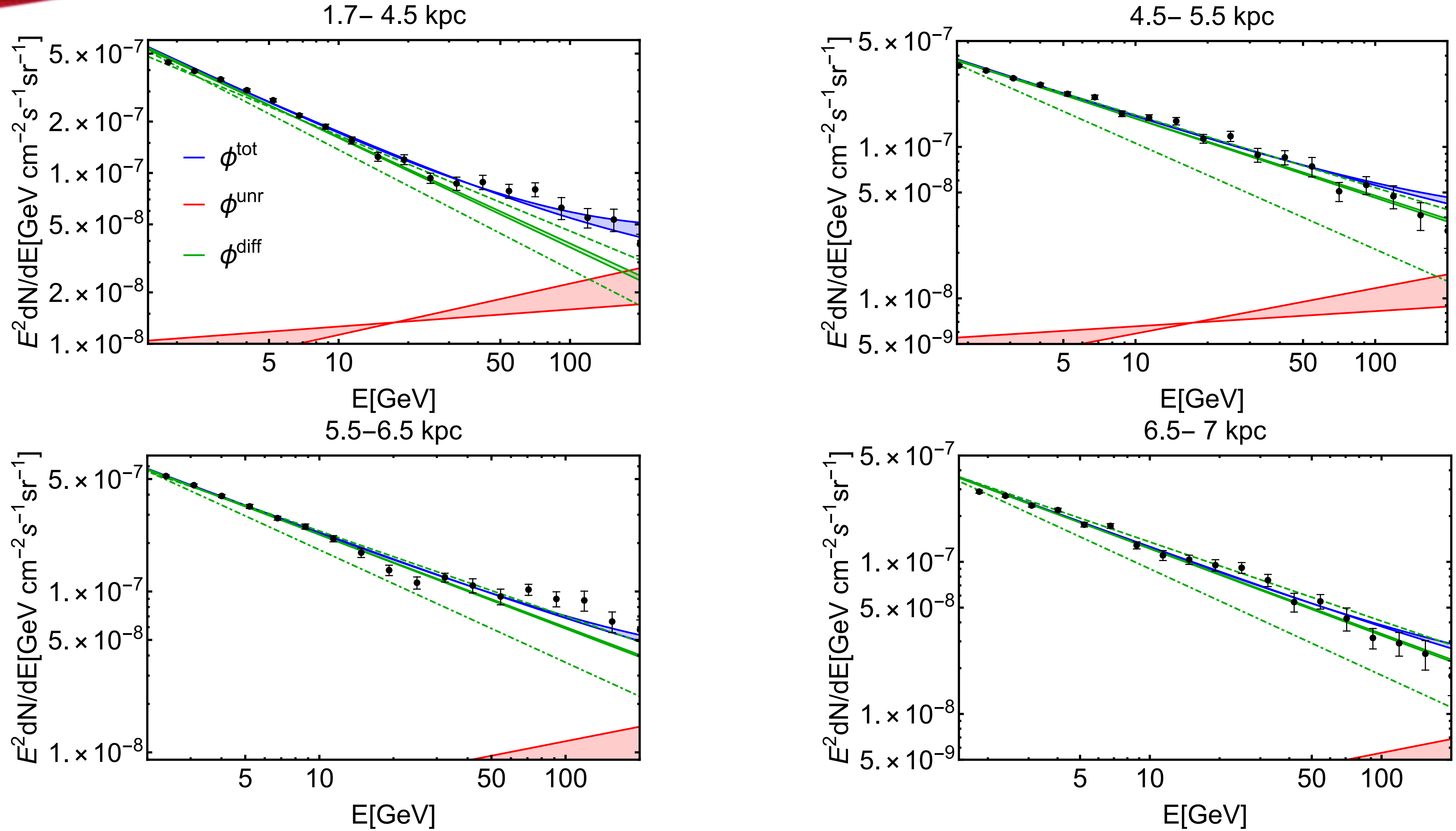

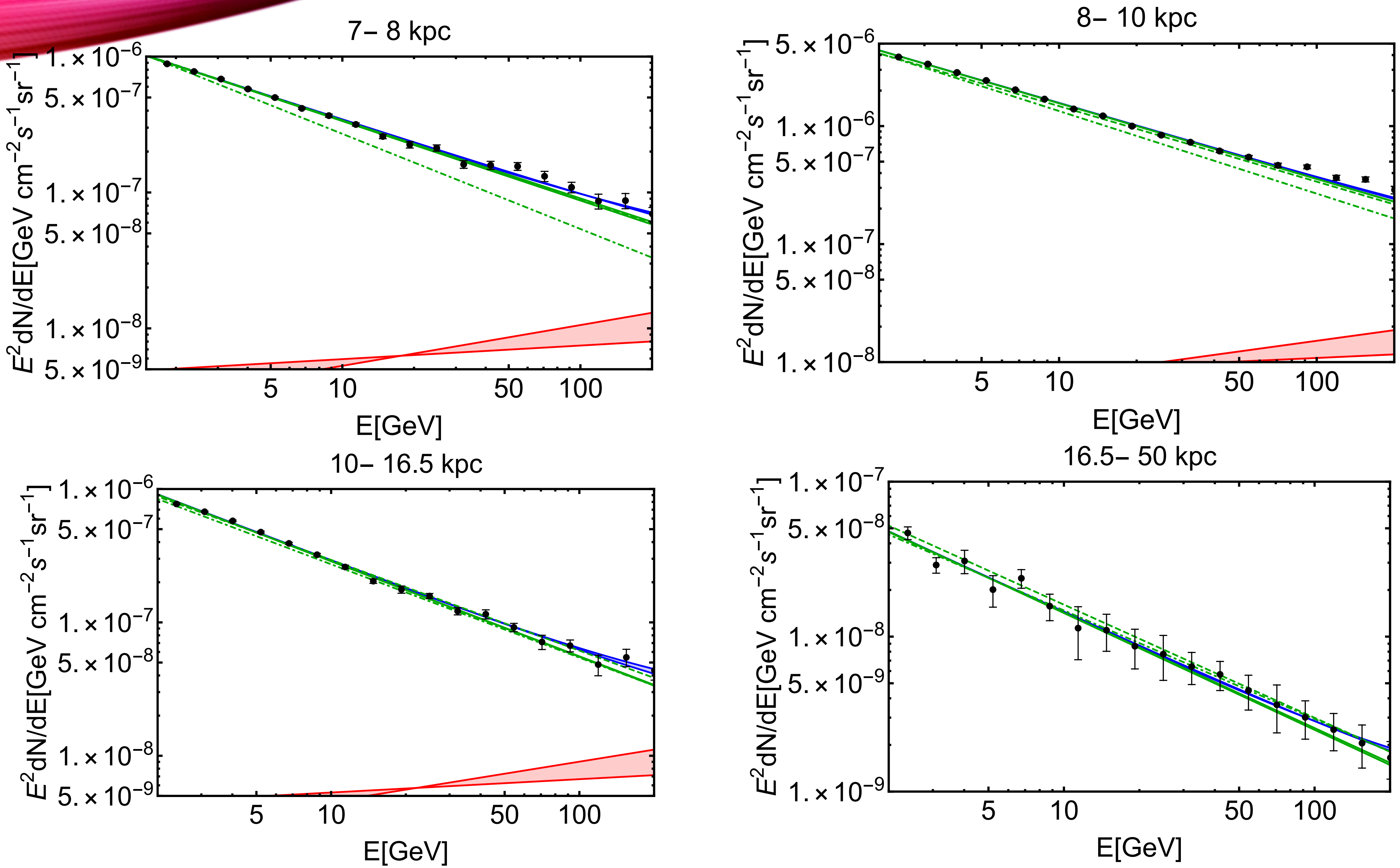

7– 8 kpc
8– 10 kpc
10– 16.5 kpc
16.5– 50 kpc
$E^2 dN/dE [GeV\ cm^{-2} s^{-1} sr^{-1}]$
E[GeV]